Clinical Oral Investigations (2021) 25:5917–5927
https://doi.org/10.1007/s00784-021-03897-6

ORIGINAL ARTICLE

Enhanced bone formation of calvarial bone defects by low-intensity pulsed ultrasound and recombinant human bone morphogenetic protein-9: a preliminary experimental study in rats

Takatomo Imafuji[1] · Yoshinori Shirakata[1] · Yukiya Shinohara[1] · Toshiaki Nakamura[1] · Kazuyuki Noguchi[1]

Received: 23 November 2020 / Accepted: 18 March 2021 / Published online: 23 March 2021
© Springer-Verlag GmbH Germany, part of Springer Nature 2021

Abstract

Objectives The aim of this study was to evaluate the combined effects of recombinant human bone morphogenetic protein - 9 (rhBMP-9) loaded onto absorbable collagen sponges (ACS) and low-intensity pulsed ultrasound (LIPUS) on bone formation in rat calvarial defects.

Materials and methods Circular calvarial defects were surgically created in 18 Wistar rats, which were divided into LIPUS-applied (+) and LIPUS-non-applied (−) groups. The 36 defects in each group received ACS implantation (ACS group), ACS with rhBMP-9 (rhBMP-9/ACS group), or surgical control (control group), yielding the following six groups: ACS (+/−), rhBMP-9/ACS (+/−), and control (+/−). The LIPUS-applied groups received daily LIPUS exposure starting immediately after surgery. At 4 weeks, animals were sacrificed and their defects were investigated histologically and by microcomputed tomography.

Results Postoperative clinical healing was uneventful at all sites. More new bone was observed in the LIPUS-applied groups compared with the LIPUS-non-applied groups. Newly formed bone area (NBA)/total defect area (TA) in the ACS (+) group (46.49 ± 7.56%) was significantly greater than that observed in the ACS (−) (34.31 ± 5.68%) and control (−) (31.13 ± 6.74%) groups ($p < 0.05$). The rhBMP-9/ACS (+) group exhibited significantly greater bone volume, NBA, and NBA/TA than the rhBMP-9/ACS (−) group (2.46 ± 0.65 mm^3 vs. 1.76 ± 0.44 mm^3, 1.25 ± 0.31 mm^2 vs. 0.88 ± 0.22 mm^2, and 62.80 ± 11.87% vs. 42.66 ± 7.03%, respectively) ($p < 0.05$). Furthermore, the rhBMP-9/ ACS (+) group showed the highest level of bone formation among all groups.

Conclusion Within their limits, it can be concluded that LIPUS had osteopromotive potential and enhanced rhBMP-9-induced bone formation in calvarial defects of rats.

Clinical relevance The use of rhBMP-9 with LIPUS stimulation can be a potential bone regenerative therapy for craniofacial/peri-implant bone defects.

Keywords Low-intensity pulsed ultrasound · Bone formation · Bone morphogenetic protein · Wound healing · Animal experiment

Introduction

The establishment of predictable bone regenerative approaches is essential for the treatment of craniofacial/peri-implant bone defects resulting from various causes, such as trauma, tumors, and peri-implantitis. Among a variety of bone regenerative procedures, local delivery of growth factors or other bioactive agents is becoming a common clinical approach because of the relative ease of use [1]. Bone morphogenetic proteins (BMPs) have been extensively reported as highly bioactive growth factors with osteoinductive potential involved in bone development and repair/regeneration [2]. In addition, it has been revealed that BMPs support distinct steps of osteoclast differentiation and activation directly and indirectly via BMP-stimulated surrounding cells by RANK/RANKL/OPG system in bone remodeling [3], and that BMP signaling acts as a mediator in osteoblast-osteoclast coupling and critically affects the rate of bone formation [3, 4]. Several animal and clinical studies have shown that topical application of recombinant human BMP-2

✉ Yoshinori Shirakata
syoshi@dent.kagoshima-u.ac.jp

[1] Department of Periodontology, Kagoshima University Graduate School of Medical and Dental Sciences, 8-35-1 Sakuragaoka, Kagoshima 890-8544, Japan

(rhBMP-2) with an absorbable collagen sponge (ACS) carrier induces marked new bone formation in various bone defects [5–13]. Indeed, a rhBMP-2/ACS product currently has four United States Food and Drug Administration (FDA)–approved clinical indications: tibial shaft fractures, spinal fusions, sinus floor elevation, and alveolar ridge augmentations [6, 8–10, 13]. The efficacy of the FDA-approved rhBMP-2/ACS has been documented in human clinical studies in both maxillary sinus floor elevation and alveolar ridge augmentation demonstrating significantly induced bone formation/maturation suitable for dental implant placement [8–10]. However, adverse side effects such as production of ectopic bone, induction of rampant inflammation, and severe edema have also been reported following high dose of rhBMP-2 application [13, 14].

On the other hand, comparative studies using adenovirus-transfection experiments to examine several BMPs revealed that BMP-9 has the greatest osteogenic potential of all BMPs, including clinically approved BMP-2 and BMP-7 [15, 16]. Interestingly, it was also demonstrated that rhBMP-9/ACS had greater osteogenic potential than surgical control or ACS alone [12, 17], and yielded new bone formation with less adipose tissues compared with rhBMP-2/ACS [12] in rat critical-sized calvarial bone defects. Furthermore, a recent in vitro study has shown that rhBMP-9 is able to promote osteoblast differentiation producing more alkaline phosphatase as well as alizarin red staining when compared to rhBMP-2 and rhBMP-7 even at 20-times lower doses [18]. Thus, rhBMP-9 may be an effective rhBMP-2 alternative for inducing bone formation at lower dosages, thereby markedly diminishing possible secondary side effects and costs associated with high-dose therapy [19].

The mechanical environment at the repair site also plays a very important role in bone healing by altering biophysical signals and vascular networks [20, 21]. Low-intensity pulsed ultrasound (LIPUS) is transmitted as an extracellular mechanical force at the cell membrane, whereby it is transduced into intracellular electrical and/or biochemical signals. This stimulus can induce various cellular events, including mesenchymal stem cell recruitment, osteoblast proliferation/differentiation, inflammation suppression, promotion of cytokine secretion, improvement of angiogenesis, extracellular matrix production, and mineralization [21–23]. In addition, several recent studies have reported that LIPUS can accelerate new bone formation in various bone defects [24, 25]. Thus, LIPUS stimulation is a clinically established, widely used, and FDA-approved intervention as noninvasive therapy to promote healing of pathological and traumatic fractures without causing untoward events [26]. Moreover, it has recently been reported that LIPUS accelerates rhBMP-2/ACS-induced bone formation in rat critical-sized femoral segmental defects [27]. These findings led to the hypothesis that rhBMP-9/ACS with LIPUS is capable of improving bone repair within short period of time after implantation in bone defects. However, it is unclear whether the combined use of LIPUS and rhBMP-9 can induce additional bone healing/regeneration in bone defects. Therefore, the aim of this study was to evaluate the combined effects of LIPUS and rhBMP-9 loaded onto ACS on bone healing/regeneration in rat calvarial defects.

Materials and methods

Experimental animals

Eighteen 17-week-old male Wistar rats (body weight: 476–497 g) were purchased from Charles River Laboratories (Kanagawa, Japan). This study was performed in accordance with ARRIVE guidelines for preclinical animal studies. All experimental protocols and procedures were approved by the Ethical Committee of the Animal Research Center of Kagoshima University, Japan (Approval No. D19011).

Surgical protocol

All animals were housed in a light- and temperature-controlled environment, and given food and water *ad libitum*. Before surgery, the experimental animals were divided into LIPUS-applied (+) and LIPUS-non-applied (−) groups containing 9 animals each per group (Fig. 1). General anesthesia was induced by a combination of an inhalation of Isoflurane® (FUJIFILM Wako Pure Chemical Co., Ltd., Osaka, Japan) and intraperitoneal injection of a mixture of 1.0 mg/mL medetomidine hydrochloride (Dorbene®vet, Kyoritsu Seiyaku Co., Tokyo, Japan), 5.0 mg/mL midazolam (Dormicum®, Astellas Pharma Inc., Tokyo, Japan), and 5.0 mg/mL butorphanol tartrate (Vetorphale®, Meiji Seika Pharma Co., Ltd., Tokyo, Japan). A local infiltration anesthesia (2%, 1:80,000 xylocaine; Fujisawa Inc., Osaka, Japan) was used at the surgical sites before surgery. The dorsal part of the cranium was shaved, and a sagittal incision of approximately 25 mm was made over the scalp of the animal. A flap was raised and 2 bone defects (2.7 mm diameter) were created on each side lateral to the sagittal plane using a slow-speed trephine bur (Stoma, Emmingen-Liptingen, Germany) with saline irrigation to prevent heat damage to the host bone. Care was also taken not to damage the dura. Four circular bone defects were created in each animal as demonstrated in Fig. 2a. To keep the regional anatomic and individual variations as low as possible, a total of 36 defects in each (LIPUS-applied (+) or LIPUS-non-applied (−)) group sequentially received cross-linked ACS (φ 2.7 mm, Colla Tape; Zimmer Dental, Carlsbad, CA, USA) with 1.0 μg rhBMP-9 (R&D Systems Minneapolis, MN, USA) implantation (rhBMP-9/ACS group), ACS implantation (ACS group), or surgical control (control group) (Fig. 1, Fig. 2b, 2c, Supplemental Table),

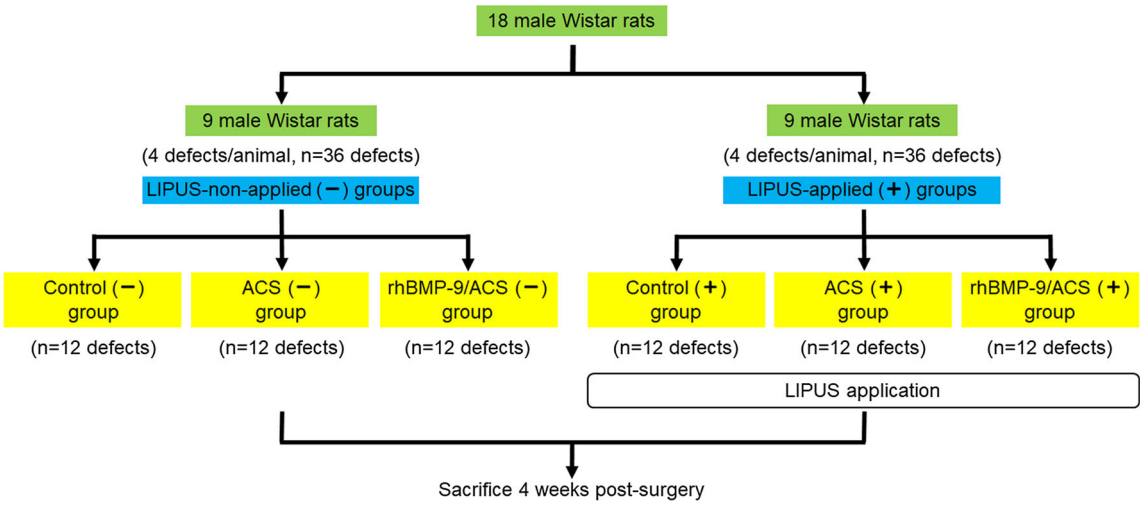

Fig. 1 The flow chart shows the study design

yielding the following six groups for evaluation: control (−), control (+), ACS (−), ACS (+), rhBMP-9/ACS (−), and rhBMP-9/ACS (+) (Fig. 1). In the ACS group**,** the ACS was loaded with sterilized water before being applied to the defect. In the rhBMP-9/ACS group, rhBMP-9 was reconstituted and diluted in sterilized water. Next, the ACS was saturated with rhBMP-9 solution and allowed to rest for 30 min prior to rhBMP-9/ACS implantation (Fig. 2b, 2c). Following implantation, the periosteum was repositioned and closed with 7-0 vicryl polyglactin sutures (Johnson & Johnson Pty Ltd., Tokyo, Japan). The skin was then closed with 6-0 Nesco Sutures (Alfresa Pharma Co., Osaka, Japan). LIPUS-applied animals (defects) were exposed to LIPUS for 20 min daily for 4 weeks. A circular transducer (20-mm diameter) was set in contact with the skin over the defect area with high viscosity gel. The transducer cable was fixed with a string to the rear of the probe to maintain stability (Fig. 2d), thus enabling precise LIPUS application to the wound via the sonicator (OSTEOTRON D2; ITO Co. Tokyo, Japan). The sonicator generated 200-μs ultrasound pulses at 1.5 MHz with a pulse repetition rate of 1.0 KHz and spatial average intensity of 30 mW/cm^2. Animals were humanely euthanized by CO_2 asphyxiation 4 weeks post-surgery (Fig. 1).

Microcomputed tomography analysis

Calvariae including the defect areas were removed and fixed in 10% neutral-buffered formalin. Formalin-fixed tissue samples were scanned with a Skyscan 1174 compact μCT (Bruker microCT, Kontich, Belgium) at 52 kV/800 μA. A Ti-0.5 filter was used to observe the whole appearance and discern the center portion of defects (including defect margin with maximum linear defect length), and obtain optimal histological sections for quantification of bone volume (BV) in defects. Three-dimensional (3D) images were constructed with the 3D creator program supplied with the instrument. A cylindrical region of interest (ROI) with a diameter of 2.7 mm and height comprising the total depth was chosen. BV at the ROI was measured using CT analyzer software (Bruker-micro CT) by a single experienced blinded examiner (T. N.).

Histologic and histomorphometric analyses

The samples were further trimmed and decalcified in EDTA solution, dehydrated, and embedded in paraffin. Serial sections of 6-μm thickness were prepared along the coronal direction. Sections were stained with hematoxylin/eosin (H&E) and

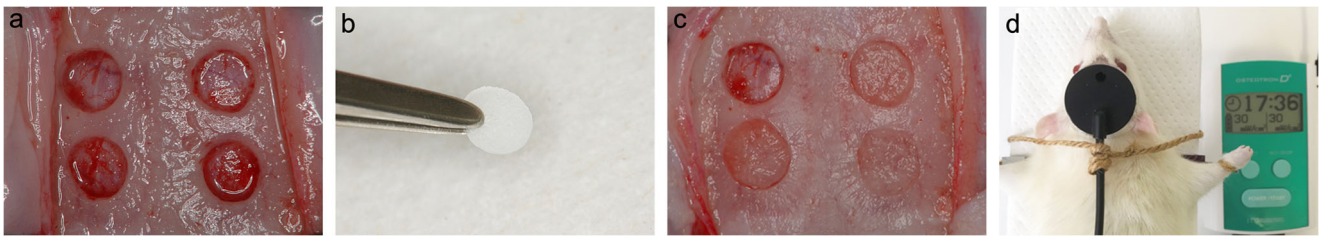

Fig. 2 **a** Four circular defects (2.7-mm diameter) were prepared using a trephine bur. **b** rhBMP-9/ACS construct before surgical implantation. **c** Each defect was assigned to the control, ACS, or rhBMP-9/ACS group. Clockwise from top left; control, ACS, rhBMP-9/ACS and rhBMP-9/ACS in the animal. **d** The transducer was applied to the skin over the defect area with high viscosity gel, and LIPUS applications were performed

examined under a light microscope (BX51; Olympus Corp., Tokyo, Japan). Images of the three most central sections of defects were taken and stored as digital files for further analysis. Measurement of the following histomorphometric parameters was performed as described in previous studies [12, 17] by one expert blinded and calibrated examiner (Yu. S.) using image processing software (Win Roof; Mitani Co., Tokyo, Japan): (1) distance between the margins of the original surgical defect (defect length: DL); (2) length of the internal bone bridging formation (defect closure: DC); (3) total defect area (TA), as determined by first identifying the external and internal surfaces of the original calvaria at the right and left margins of the surgical defect, and then connecting them with lines drawn along their respective curvatures; (4) region stained with H&E in the TA, which was color extracted and defined as the newly formed bone area (NBA); and (5) vertical augmentation height as measured at four points, two at 0.54 mm apart in the center of the defect and two at 0.54 mm internally from the defect margins, with each pair of measurements averaged to yield the mean central bone height (CBH) and marginal bone height (MBH). These heights were composed of calcified osseous tissue, grafted biomaterial, and/or the soft tissue interface. TA and NBA were measured in square millimeters (mm^2), and NBA was calculated as a percentage of the TA. The linear measurement of DC was calculated as the percentage of the defect length within each defect. Intra-examiner reliability was assessed by repeating the measurements on randomly selected 10% samples of all images 48 h after the initial examination. Calibration was accepted if measurements at baseline and at 48 h later were similar at the>90% level.

Statistical analysis

The bone defect was regarded as the statistical unit. The primary outcome of this study was the histomorphometric outcome in terms of NBA in particular, measured for six treatment groups at 4 weeks. Due to the limited number of similar studies with a comparable design and the primary outcome, no specific power analysis for sample calculation was performed. One-way analysis of variance (ANOVA) was used to compare data among groups. When the ANOVA was significant, Bonferroni's post hoc test was performed for multiple comparisons. A P value of <0.05 was considered statistically significant. Statistical analyses were performed using statistical software (BellCurve for Excel, Social Survey Research Information Co., Ltd., Tokyo, Japan). All results are expressed as mean ± SD.

Results

Clinical outcomes

Postoperative healing was uneventful in all animals. No visible complications, such as wound dehiscence, infection, or suppuration, were observed during the entire 4-week healing period.

μCT analysis

Representative 3D μCT images are shown in Fig. 3. Overall, LIPUS-applied (+) groups exhibited developed ossification compared with LIPUS-non-applied (−) groups. Microradiographical analysis demonstrated broad radiolucent areas in the control (−) group (Fig. 3a). In the control (+) group, some bone formation occurred from the margin of defects to varying degrees (Fig. 3b). Similar to the control (−) group, the ACS (−) group showed broad radiolucent areas in the defects (Fig. 3c). On the other hand, an increase in the radiopacity within defects was observed in the ACS (+) group (Fig. 3d). Although some radiolucent regions remained in the rhBMP-9/ACS (−) group (Fig. 3e), a great increase in the radiopacity within defects was observed. In contrast, the rhBMP-9/ACS (+) group (Fig. 3f) exhibited homogenous radiopacity in the whole defect areas compared with the rhBMP-9/ACS (−) group. BV measurement revealed higher values in LIPUS-applied groups compared with LIPUS-non-applied groups. Furthermore, BV in the rhBMP-9/ACS (+) group (2.46 ± 0.65 mm^3) was significantly higher compared with control (−) (1.17 ± 0.39 mm^3, $P < 0.01$), ACS (−) (1.28 ± 0.60 mm^3, $P < 0.01$), rhBMP-9/ACS (−) (1.76 ± 0.44 mm^3, $P < 0.05$), control (+) (1.63 ± 0.58 mm^3, $P < 0.01$), and ACS (+) (1.76 ± 0.62 mm^3, $P < 0.05$) groups (Fig. 4).

Histomorphological descriptions

At 4 weeks, no abnormal infiltration of inflammatory cells was observed in the healed defects. New bone formation in the control (−) group was mostly restricted to areas close to the original borders of defects (Fig. 5a). Most defects in the control (−) group were occupied by connective tissue composed of large numbers of collagen fibers parallel to the wound defect (Fig. 5a, Fig. 6a). However, the control (+) group exhibited varying degrees of slender bone growth from both edges to the center of defects (Fig. 5b). More osteoblast-like cells were observed around the bony rims of defects in the control (+) group compared with the control (−) group (Fig. 6a, 6b). Connective tissue in the central portions of defects in control (−) and control (+) groups was visibly thinner than the original calvaria (Fig. 5a, 5b). The volume and contour of the defect area in ACS applied groups maintained the original shapes of calvariae compared with control (−) and control (+) groups (Fig. 5c–f). In the ACS (−) group, newly formed bone with osteoblasts and osteocytes was evident, mainly at the periphery of defects, and most defects were considerably occupied by connective tissue and small ACS fragments (Fig. 5c, Fig. 6c). Histologic findings observed in the ACS (+) group were similar, however, with more new bone formation visibly

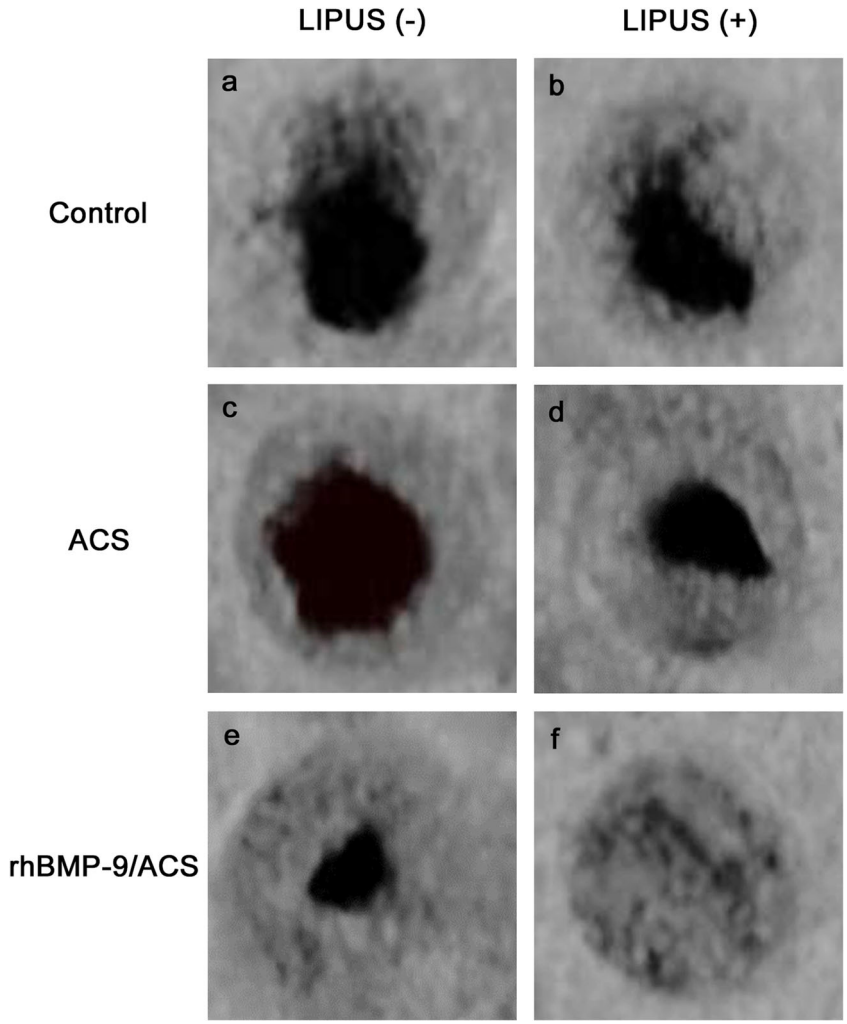

Fig. 3 Three-dimensionally reconstructed radiographic images of representative rat calvarial bone defects after 4 weeks of healing. **a** Control (-), **b** control (+), **c** ACS (-), **d** ACS (+), **e** rhBMP-9/ACS (-), and **f** rhBMP-9/ACS (+)

occupying the defects (Fig. 5d). The ACS (+) group exhibited more potent formation of calcified areas compared with the ACS (−) group (Fig. 5d, Fig. 6d). Specimens in the rhBMP-9-applied (+/−) groups showed a more advanced stage of remodeling and consolidation of bone compared with control (+/−) and ACS (+/−) groups. The structure and thickness of new bone were similar in rhBMP-9/ACS (+/−) groups, but the rhBMP-9/ACS (+) group exhibited a tendency to form more

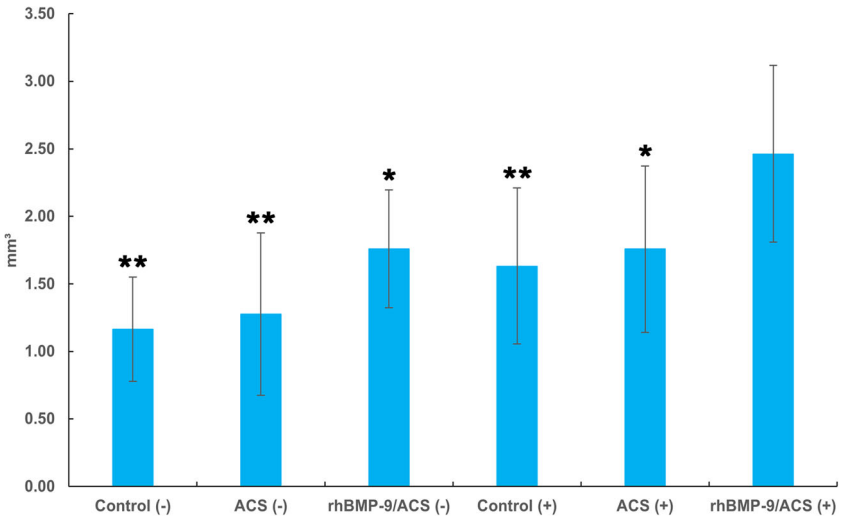

Fig. 4 Bone volume (mm^3) for each treatment group in rat calvarial bone defects at 4 weeks. * Statistically significant difference compared to the rhBMP-9/ACS (+) group ($P < 0.05$); ** Statistically significant difference compared to the rhBMP-9/ACS (+) group ($P < 0.01$)

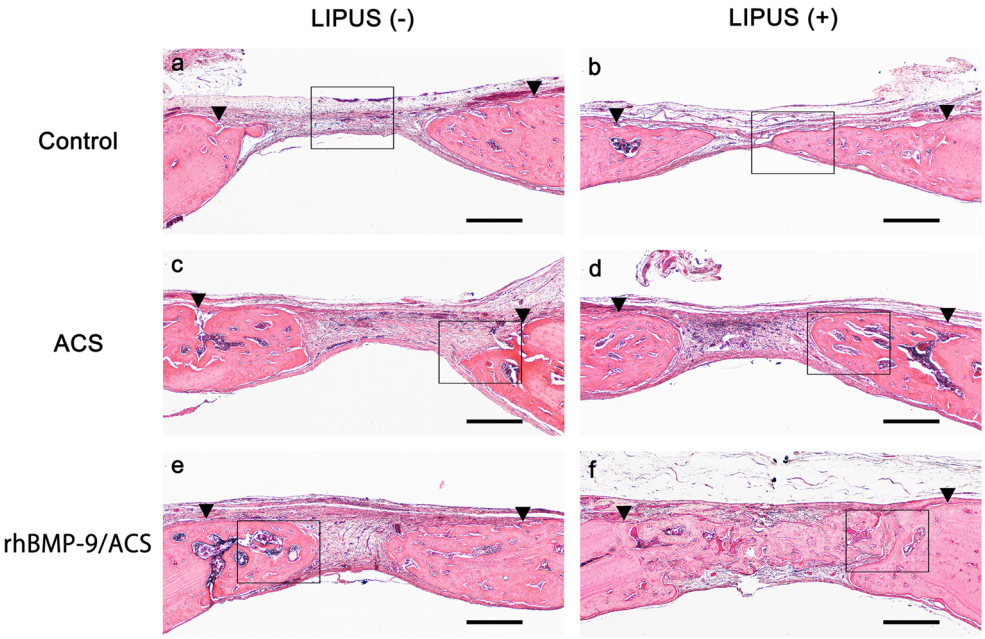

Fig. 5 Representative histologic photomicrographs of rat calvarial bone defects at 4 weeks post-surgery. Overview of defect sites treated with **a** control (-), **b** control (+), **c** ACS (-), **d** ACS (+), **e** rhBMP-9/ACS (-), and **f** rhBMP-9/ACS (+). Arrow head: defect margin (scale bar, 500 μm; hematoxylin and eosin stain)

mineralized bone containing abundant lacuna consisting of many osteocytes and blood vessels (Fig. 5f, Fig. 6f) than the rhBMP-9 (−) group (Fig. 5e, Fig. 6d). Furthermore, newly formed bone was almost integrated with the original bone in the rhBMP-9/ACS (+) group (Fig. 6f, Fig. 7).

Histomorphometric analysis

The results of histomorphometric analysis are shown in Table 1. The values of the histomorphometric parameters in LIPUS-applied (+) groups were in general greater than that in

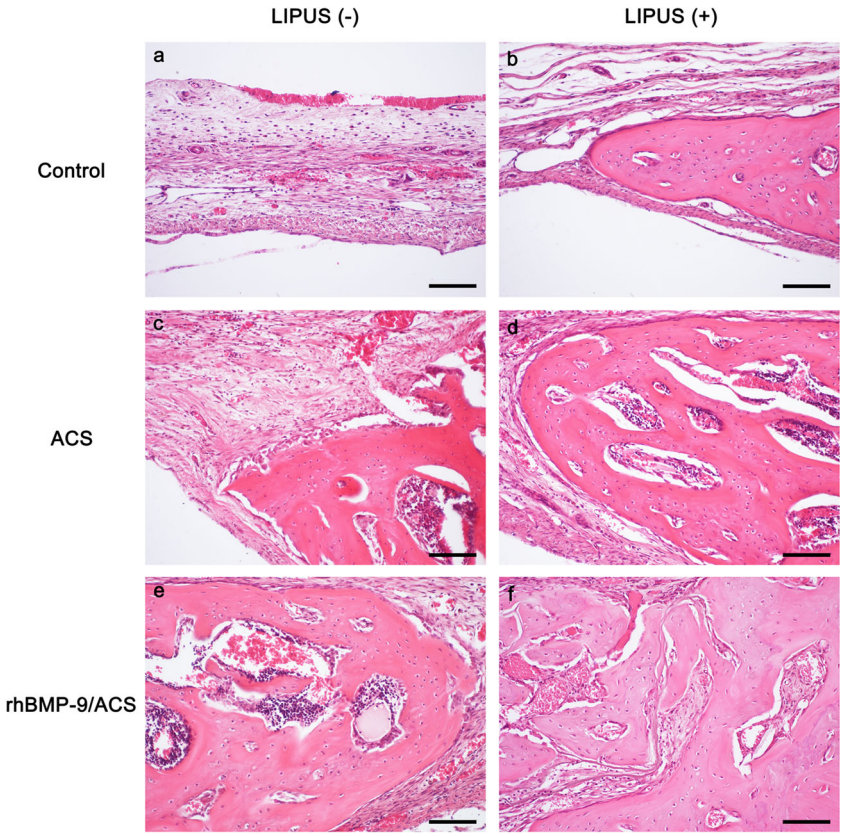

Fig. 6 Representative histologic photomicrographs of rat calvarial bone defects at 4 weeks post-surgery. Higher magnification of the framed area in Fig. 5a (**a**), 5b (**b**), 5c (**c**), 5d (**d**), 5e (**e**), and 5f (**f**). (Scale bar, 100 μm; hematoxylin and eosin stain)

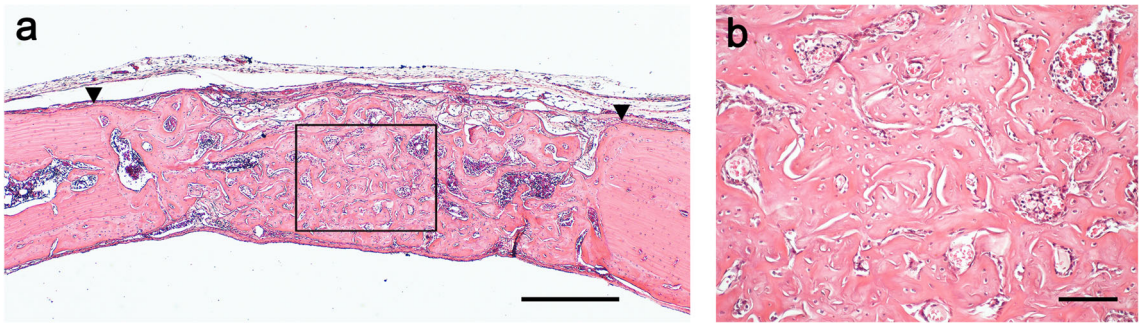

Fig. 7 **a** Histologic overview of a completely healed bone defect in the rhBMP-9/ACS (+) group (scale bar, 500 μm; hematoxylin and eosin stain). Arrow head: defect margin. **b** Higher magnification of a center portion of the defect (scale bar, 100 μm; hematoxylin and eosin stain). New bone formation occurred from both margins of the defects, and bone bridging occurred across the entire defect

LIPUS-non-applied (−) groups. DC and DC/DL in the rhBMP-9/ACS (−) group were significantly greater than that observed in the control (−) group ($P < 0.01$) and ACS (−) group ($P < 0.05$). The rhBMP-9/ACS (+) group demonstrated significantly higher levels of DC (2.37 ± 0.32 mm) and DC/DL (87.10 ± 11.83%) compared with control (−), ACS (−), control (+), and ACS (+) groups ($P < 0.01$). Regenerated augmentation heights (CBH and MBH) were significantly lower in the control groups (both LIPUS-non-applied and LIPUS-applied) compared with the other groups ($P < 0.05$). NBA and NBA/TA in the rhBMP-9/ACS (−) group were significantly increased compared with the control (−) group ($P < 0.05$). NBA/TA in the ACS (+) group was significantly increased compared with control (−) and ACS −) groups ($P < 0.01$). The rhBMP-9/ACS (+) group showed the highest levels of NBA and NBA/TA (1.25 ± 0.31 mm^2, 62.80 ± 11.87%), which were significantly higher than those observed in the other treatment groups. In four of the 12 rhBMP-9/ACS (+) specimens, complete closure of the defect was observed (Fig. 7). Moreover, the number of animals that exhibited substantial bone formation was higher in the rhBMP-9/ACS (+) group compared with other groups (Table 2).

Table 1 Histomorphometric linear and area measurements in each treatment group ($n = 12$ defects)

Surgical treatment							
Histometric parameter	LIPUS (−) (1) Control ($n = 12$)	(2) ACS ($n = 12$)	(3) rhBMP-9/ACS ($n = 12$)	LIPUS (+) (4) Control ($n = 12$)	(5) ACS ($n = 12$)	(6) rhBMP-9/ACS ($n = 12$)	Statistically significant differences
DL (mm)	2.72 ± 0.01	2.72 ± 0.02	2.71 ± 0.01	2.73 ± 0.03	2.72 ± 0.01	2.72 ± 0.01	NS
DC (mm)	1.50 ± 0.22	1.53 ± 0.18	2.01 ± 0.39	1.76 ± 0.50	1.83 ± 0.29	2.37 ± 0.32	(1)(2) vs. (3)* (1)(2)(4)(5) vs. (6)**
DC/DL (%)	55.14 ± 8.29	56.39 ± 6.78	74.09 ± 14.13	64.42 ± 18.21	67.41 ± 10.51	87.10 ± 11.83	(1)**(2)* vs. (3) (1)(2)(4)(5) vs. (6)**
CBH (mm)	0.68 ± 0.14	1.00 ± 0.27	1.17 ± 0.31	0.64 ± 0.11	0.99 ± 0.22	1.17 ± 0.28	(1) vs. (2)*(3)** (5)*(6)** (4)** vs. (2)(3)(5)(6)
MBH (mm)	1.21 ± 0.18	1.47 ± 0.26	1.50 ± 0.23	1.08 ± 0.13	1.34 ± 0.19	1.52 ± 0.19	(1) vs. (2)*(3)*(6)** (4) vs. (2)**(3)**(5)*(6)**
TA (mm^2)	1.93 ± 0.21	1.95 ± 0.26	2.03 ± 0.23	1.81 ± 0.11	1.80 ± 0.19	1.98 ± 0.21	NS
NBA (mm^2)	0.60 ± 0.15	0.67 ± 0.17	0.88 ± 0.22	0.69 ± 0.17	0.84 ± 0.17	1.25 ± 0.31	(1) vs (3)* (1)(2)(3)(4)(5) vs. (6)**
NBA/TA (%)	31.13 ± 6.74	34.31 ± 5.68	42.66 ± 7.03	38.61 ± 9.17	46.49 ± 7.56	62.80 ± 11.87	(1) vs. (3)*(5)** (2) vs. (5)** (1)(2)(3)(4)(5) vs. (6)**

Values are presented as mean ± standard deviation. LIPUS, low-intensity pulsed ultrasound; ACS, absorbable collagen sponge; rhBMP-9, recombinant human BMP-9; DL, defect length; DC, defect closure; CBH, central bone height; MBH, marginal bone height; TA, total defect area, NBA, newly formed bone area; NS: not significant *Statistically significant differences ($P < 0.05$) ** Statistically significant differences ($P < 0.01$).

Discussion

This study aimed to investigate the effect of combining rhBMP-9 and LIPUS on bone formation in rat calvarial bone defects. The results revealed that (i) LIPUS-applied groups showed more new bone formation compared with LIPUS-non-applied groups, (ii) rhBMP-9/ACS applied groups demonstrated much greater new bone formation than the four groups without rhBMP-9 application, and (iii) the additional application of LIPUS to rhBMP-9/ACS led to the highest level of bone formation among all treatment groups.

In the LIPUS-applied control group, new bone formation was observed with superior effectiveness in terms of DC and DC/DL compared with the LIPUS-non-applied control group, although no statistically significant differences were detected between these groups. In addition, more osteoblast-like cells were observed around the extended bony rim in the control (+) group compared with the control (−) group. The ACS (+) group also exhibited a statistically higher level of NBA/TA compared with the ACS (−) group. These results are similar to a previous report indicating significantly greater increases in bone volume of original calvarial defects in LIPUS-applied rats (18.9%) compared with LIPUS-non-applied rats (9.8%), as well as clear bone labeling in the edges of newly formed bone in LIPUS-applied defects at 4 weeks [24]. Furthermore, Jung et al. [28] reported that new bone formation was enhanced by about 20% in the LIPUS-applied group relative to the LIPUS-non-applied control group; moreover, the LIPUS group exhibited thicker new bone tissue and more osteocytes than the control group in rat calvarial defects after 8 weeks. These findings are supported by *in vitro* studies showing that LIPUS stimulation significantly promoted the proliferation of osteoblasts [22, 29, 30] and bone marrow-derived mesenchymal stem cells [23, 31], and increased expression of cyclooxygenase 2 and runt-related transcription factor 2, early response genes involved in the process of osteoblast differentiation [32–34]. Furthermore, LIPUS has been shown to enhance the expression of osteogenic genes (e.g., BMP-2, -4, and -7, osteopontin, osteonectin, and osteocalcin) produced by osteoblasts and various cells [29, 30, 32, 33, 35, 36] and stimulate the production of angiogenic cytokine vascular endothelial growth factor [37]. Additionally, a very recent study has found that LIPUS significantly upregulates protein levels of BMP-2 and phospho-Smad 1/5/9 in murine periosteum–derived cells [38]. Thus, the effects of LIPUS might enhance bone formation in rat calvarial defects.

rhBMP-9/ACS–applied groups demonstrated more new bone formation compared with the four groups without rhBMP-9 application. These results are consistent with our previous studies of rat calvarial bone defects [12, 17], which reported that rhBMP-9 combined with ACS significantly promoted bone formation compared with clot or ACS alone. Furthermore, our positive results following rhBMP-9 application are similar to the previous studies examining combinations of collagen membranes with rhBMP-9 [39] or bovine-derived natural bone mineral particles with rhBMP-9 [40], which significantly promoted osteogenic differentiation of osteoprogenitor cells and elicited higher osteoblast gene expression, alkaline phosphatase activity, and Alizarin Red staining compared with the respective material controls alone [39, 40]. It is currently understood that BMP-9-mediated osteogenesis occurs via overlapping yet unique pathways from other BMPs including BMP-2 [19]. Previous reports have indicated that BMP-9 induces osteoblastic differentiation of mesenchymal stem cells through the Notch pathway [41, 42], Wnt/β-catenin pathway [41, 43], peroxisome proliferator–activated receptor γ pathway [41, 44], retinoid acid signaling pathway [41], transforming growth factor β/Smad-1/5/8 [41, 45] and the mitogen-activated protein kinase pathways [45, 46], and directly induces rapid phosphorylation of glycogen synthase kinase 3 beta, leading to the accumulation of β-catenin in a Wnt-independent manner through the class I phosphoinositide 3 kinase-Akt axis in osteoblasts [47]. Interestingly, several studies have also demonstrated that

Table 2 Summary of histological classifications of bone closure at 4 weeks post-surgery

Surgical treatment		Degree of defect closure		
		Partial (40–60%)	Intermediate (61–80%)	Substantial (81–100%)
LIPUS (-)	Control (−)	7/12	5/12	0/12
	ACS (−)	9/12	3/12	0/12
	rhBMP-9/ACS (−)	1/12	8/12	3/12
LIPUS (+)	Control (+)	5/12	4/12	3/12
	ACS (+)	3/12	7/12	2/12
	rhBMP-9/ACS (+)	0/12	5/12	7/12

Data are shown as frequency observations/specimens (sites).

LIPUS, low-intensity pulsed ultrasound; ACS, absorbable collagen sponge: rhBMP-9, recombinant human BMP-9

BMP-9 shows complete resistance to noggin, an extracellular antagonist that binds and blocks SMAD-dependent signaling and inhibits BMP-2-induced bone formation [19, 48, 49]. Furthermore, BMP-3, a known inhibitor of BMP-2- and BMP-7-mediated osteogenesis, does not inhibit BMP-9-mediated bone formation [16, 19]. Although the molecular mechanisms of rhBMP-9-induced osteogenesis are not yet fully elucidated, accumulating observations and promising evidence suggest that rhBMP-9 plays predominant role as a rapid and potent inducer of bone formation. The results of μCT analysis revealed that the rhBMP-9/ACS (+) group had a significantly higher BV compared with the other five groups, as well as the highest levels of DC, DC/DL, NBA, and NBA/TA. In particular, DC/DL of the rhBMP-9/ACS (+) group (87.10% ± 11.83%) was greater than that of the lactoferrin-permeated ACS applied group (73.3% ± 19.1%) in non-critical-sized rat calvarial defects (2.7-mm diameter) at 4 weeks [50]. Furthermore, statistically significant differences in NBA and NBA/TA were found between rhBMP-9/ACS (+) and rhBMP-9/ACS (−) groups. These findings suggest that LIPUS is able to support callus maturation at low dosage (1 μg/site) of rhBMP-9, and enhanced rhBMP-9-induced bone formation at an early period of wound healing. The great osteogenic potential of rhBMP-9/ACS (+) group is explained by the presence of specific receptors and crosstalk with various cells and the aforementioned BMP-related pathways associated with LIPUS and rhBMP-9 stimulation. Thus, it is likely that the combined use of LIPUS and rhBMP-9/ACS may become a novel promising approach for bone regeneration/augmentation in peri-implant bone defects.

Nevertheless, the present study had several limitations. Previous animal studies have demonstrated that the rat calvarial bone defect is a convenient experimental model because of high reproducibility for evaluating the efficacy of osteopromotive materials/agents in stimulating bone healing [12, 17, 24, 28, 50, 51] and a 2.7-mm calvarial bone defect is not critical but not completely healed by clot alone within 4 weeks [24, 50, 51]. Furthermore, rapid bone formation was expected following rhBMP-9/ACS and LIPUS application in this study. Thus, as a novel experimental design, multiple non-critical-size bone defects were created in an experimental animal for a short observation period to simultaneously evaluate several treatment modalities (i.e., clot alone, ACS, and rhBMP-9/ACS with/without LIPUS application) to determine their effects on bone formation. However, the present results were obtained in the small number of animals/defects without internal comparison in the same animal with/without LIPUS, and possible biologic interactions of each treatment were not completely excluded. In addition, the results may not be directly applicable to intraoral sites since the surgical area in rat calvaria is isolated from oral flora [51, 52]. Consequently, further studies including alveolar bone defects in a larger number of large animals and different periods of wound healing are required to thoroughly evaluate effects on the bone healing process. In addition, *in vitro* studies to elucidate the mechanisms governing cell behavior by which rhBMP-9 and LIPUS induced bone formation and histochemical and immunohistochemical methods for evaluating bone maturation/metabolism are needed prior their clinical application in craniofacial/peri-implant bone defects in humans.

Conclusion

Within their limits, it can be concluded that LIPUS had osteopromotive potential and enhanced rhBMP-9-induced bone formation in calvarial defects of rats.

Supplementary Information The online version contains supplementary material available at https://doi.org/10.1007/s00784-021-03897-6.

Acknowledgements We thank Edanz Group (https://en-author-services.edanzgroup.com/ac) for editing a draft of this manuscript.

Funding This study was supported by Grants-in-Aid for Scientific Research C (No. 19 K10169) and Grant-in-Aid for Young Scientists (No. 18 K17089) from the Japan Society for the Promotion of Science.

Declarations

Ethics approval The experimental protocol was reviewed and approved by the ethical committee of the Animal Research Center of Kagoshima University, Japan (Approval No. D19011). This study conformed to the ARRIVE guidelines for preclinical animal studies.

Informed consent For this kind of study, formal consent is not required.

Conflict of interest The authors declare that they have no conflict of interest.

References

1. Lieberman JR, Daluiski A, Einhorn TA (2002) The role of growth factors in the repair of bone. Biology and clinical applications. J Bone Joint Surg Am 84:1032–1044
2. Deschaseaux F, Sensebe L, Heymann D (2009) Mechanisms of bone repair and regeneration. Trends Mol Med 15:417–429
3. Lademann F, Hofbauer LC, Rauner M (2020) The bone morphogenetic protein pathway: the osteoclastic perspective. Front Cell Dev Biol 8:586031. https://doi.org/10.3389/fcell.2020.586031 eCollection 2020
4. Abe E, Yamamoto M, Taguchi Y, Lecka-Czernik B, O'Brien CA, Economides AN, Stahl N, Jilka RL, Manolagas SC (2000) Essential requirement of BMPs-2/4 for both osteoblast and osteoclast formation in murine bone marrow cultures from adult mice: antagonism by noggin. J Bone Miner Res 15:663–673
5. Fiorellini JP, Howell TH, Cochran D, Malmquist J, Lilly LC, Spagnoli D, Toljanic J, Jones A, Nevins M (2005) Randomized study evaluating recombinant human bone morphogenetic

protein-2 for extraction socket augmentation. J Periodontol 76: 605–613
6. McKay WF, Peckham SM, Badura JM (2007) A comprehensive clinical review of recombinant human bone morphogenetic protein-2 (INFUSE® Bone Graft). Int Orthop 31:729–734
7. Herford AS, Boyne PJ (2008) Reconstruction of mandibular continuity defects with bone morphogenetic protein-2 (rhBMP-2). J Oral Maxillofac Surg 66:616–624
8. Triplett RG, Nevins M, Marx RE, Spagnoli DB, Oates TW, Moy PK, Boyne PJ (2009) Pivotal, randomized evaluation of recombinant human bone morphogenetic protein-2/absorbable collagen sponge and autogenous bone graft for maxillary sinus floor augmentation. J Oral Maxillofac Surg 67:1947–1960
9. Katanec D, Granić M, Majstorović M, Trampus Z, Pandurić DG (2014) Use of recombinant human bone morphogenetic protein (rhBMP2) in bilateral alveolar ridge augmentation: case report. Coll Antropol 38:325–330
10. de Freitas RM, Susin C, Tamashiro WM, Chaves de Souza JA, Marcantonio C, Wikesjö UM, Pereira LA, Marcantonio E Jr (2016) Histological analysis and gene expression profile following augmentation of the anterior maxilla using rhBMP-2/ACS versus autogenous bone graft. J Clin Periodontol 43:1200–1207
11. Ben Amara H, Lee JW, Kim JJ, Kang YM, Kang EJ, Koo KT (2017) Influence of thBMP-2 on guided bone regeneration for placement and functional loading of dental implants: a radiographic and histologic study in dogs. Int J Oral Maxillofac Implants 32: e265–ee27
12. Nakamura T, Shirakata Y, Shinohara Y, Miron RJ, Hasegawa-Nakamura K, Fujioka-Kobayashi M, Noguchi K (2017) Comparison of the effects of recombinant human bone morphogenetic protein -2 and -9 on bone formation in rat calvarial critical -size defects. Clin Oral Investig 21:2671–2679
13. Grey ZJ, Howie RN, Durham EL, Hall SR, Helke KL, Steed MB, LaRue AC, Muise-Helmericks RC, Cray JJ (2019) Sub-clinical dose of bone morphogenetic protein-2 does not precipitate rampant, sustained inflammatory response in bone wound healing. Wound Repair Regen 27:335–344
14. Zara JN, Siu RK, Zhang X, Shen J, Ngo R, Lee M, Li W, Chiang M, Chung J, Kwak J, Wu BM, Ting K, Soo C (2011) High doses of bone morphogenetic protein 2 induce structurally abnormal bone and inflammation in vivo. Tissue Eng Part A 17:1389–1399
15. Cheng H, Jiang W, Phillips FM, Haydon RC, Peng Y, Zhou L, Luu HH, An N, Breyer B, Vanichakarn P, Szatkowski JP, Park JY, He TC (2003) Osteogenic activity of the fourteen types of human bone morphogenetic proteins (BMPs). J Bone Joint Surg Am 85:1544–1552
16. Kang Q, Sun MH, Cheng H, Peng Y, Montag AG, Deyrup AT, Jiang W, Luu HH, Luo J, Szatkowski JP, Vanichakarn P, Park JY, Li Y, Haydon RC, He TC (2004) Characterization of the distinct orthotopic bone-forming activity of 14 BMPs using recombinant adenovirus-mediated gene delivery. Gene Ther 11:1312–1320
17. Shinohara Y, Nakamura T, Shirakata Y, Noguchi K (2016) Bone healing capabilities of recombinant human bone morphogenetic protein-9 (rhBMP-9) with a chitosan or collagen carrier in rat calvarial defects. Dent Mater J 35:454–460
18. Fujioka-Kobayashi M, Abd EL Raouf M, Saulacic N, Kobayashi E, Zhang Y, Schaller B, Miron RJ (2018) Superior bone-inducing potential of rhBMP9 compared to rhBMP2. J Biomed Mater Res A 106:1561–1574
19. Miron RJ, Nakamura T, Shirakata Y, Saulacic N, Noguchi K, Zhang Y, Fujioka-Kobayashi M (2019) Next-generation bone morphogenetic protein 9: the future of bone regeneration? In: Miron RJ, Zhang Y (eds) Next-Generation biomaterials for bone & periodontal regeneration, 1st edn. Quintessence Publishing Co Inc, Batavia, pp 255–264
20. Bolander ME (1992) Regulation of fracture repair by growth factors. Proc Soc Exp Biol Med 200:165–170
21. Boerckel JD, Uhring BA, Willett NJ, Huebsch N, Guldberg RE (2011) Mechanical regulation of vascular growth and tissue regeneration in vivo. Proc Natl Acad Sci U S A 108:E674–E680
22. Doan N, Reher P, Meghji S, Harris M (1999) In vitro effects of therapeutic ultrasound on cell proliferation, protein synthesis, and cytokine production by human fibroblasts, osteoblasts, and monocytes. J Oral Maxillofac Surg 57:409–419
23. Uddin SM, Qin YX (2013) Enhancement of osteogenic differentiation and proliferation in human mesenchymal stem cells by a modified low intensity ultrasound stimulation under simulated microgravity. PLoS One 8:e73914
24. Hasuike A, Sato S, Udagawa A, Ando K, Arai Y, Ito K (2011) In vivo bone regenerative effect of low-intensity pulsed ultrasound in rat calvarial defects. Oral Surg Oral Med Oral Pathol Oral Radiol Endod 111:e12–e20
25. Shirakata Y, Imafuji T, Sena K, Shinohara Y, Nakamura T, Noguchi K (2020) Periodontal tissue regeneration after low-intensity pulsed ultrasound stimulation with or without intramarrow perforation in two-wall intra-bony defects -A pilot study in dogs. J Clin Periodontol 47:54–63
26. Busse JW, Bhandari M, Kulkami AV, Tunks E (2002) The effect of low-intensity pulsed ultrasound therapy on time to fracture healing: a meta-analysis. CMAJ 166:437–441
27. Angle SR, Sena K, Sumner DR, Virkus WW, Virdi AS (2014) Combined use of low-intensity pulsed ultrasound and rhBMP-2 to enhance bone formation in a rat model of critical size defect. J Orthop Trauma 28:605–611
28. Jung YJ, Kim R, Ham HJ, Park SI, Lee MY, Kim J, Hwang J, Park MS, Yoo SS, Maeng LS, Chang W, Chung YA (2015) Focused low-intensity pulsed ultrasound enhances bone regeneration in rat calvarial bone defect through enhancement of cell proliferation. Ultrasound Med Biol 41:999–1007
29. Suzuki A, Takayama T, Suzuki N, Kojima T, Ota N, Asano S, Ito K (2009) Daily low-intensity pulsed ultrasound stimulates production of bone morphogenetic protein in ROS 17/2.8 cells. J Oral Sci 51: 29–36
30. Suzuki A, Takayama T, Suzuki N, Sato M, Fukuda T, Ito K (2009) Daily low-intensity pulsed ultrasound-mediated osteogenic differentiation in rat osteoblasts. Acta Biochim Biophys Sin 41:108–115
31. Ling L, Wei T, He L, Wang Y, Wang Y, Feng X, Zhang W, Xiong Z (2017) Low-intensity pulsed ultrasound activates ERK1/2 and PI3K-Akt signaling pathway and promotes the proliferation of human amnion-derived mesenchymal stem cells. Cell Prolif 50: e12383
32. Warden SJ, Favaloro JM, Bennell KL, McMeeken JM, Ng KW, Zajac JD, Wark JD (2001) Low-intensity pulsed ultrasound stimulates a bone-forming response in UMR-106 cells. Biochem Biophys Res Commun 286:443–450
33. Sena K, Leven RM, Mazhar K, Sumner DR, Virdi AS (2005) Early gene response to low-intensity pulsed ultrasound in rat osteoblastic cells. Ultrasound Med Biol 31:703–708
34. Takayama T, Suzuki N, Ikeda K, Shimada T, Suzuki A, Maeno M, Otsuka K, Ito K (2007) Low-intensity pulsed ultrasound stimulates osteogenic differentiation in ROS 17/2.8 cells. Life Sci 80:965–971
35. Fávaro-Pípi E, Bossini P, de Oliveira P, Ribeiro JU, Tim C, Parizotto NA, Alves JM, Ribeiro DA, de Araujo HSS, Renno ACM (2010) Low-intensity pulsed ultrasound produced an increase of osteogenic genes expression during the process of bone healing in rats. Ultrasound Med Biol 36:2057–2064
36. San'Anna EF, Leven RM, Virdi AS, Sumner DR (2005) Effect of low-intensity pulsed ultrasound and BMP-2 on rat bone marrow stromal cell gene expression. J Orthop Res 23:646–652

37. Reher P, Doan N, Bradnock B, Meghji S, Harris M (1999) Effect of ultrasound on the production of IL-8, basic FGF and VEGF. Cytokine 11:416–423
38. Maung WM, Nakata H, Miura M, Miyasaka M, Kim YK, Kasugai S, Kuroda S (2020) Low-intensity pulsed ultrasound stimulates osteogenic differentiation of periosteal cells in vitro. Tissue Eng Part A. https://doi.org/10.1089/ten.TEA.2019.0331
39. Fujioka-Kobayashi M, Sawada K, Kobayashi E, Schaller B, Zhang Y, Miron RJ (2016) Recombinant human bone morphogenetic protein 9 (rhBMP9) induced osteoblastic behavior on a collagen membrane compared with rhBMP2. J Periodontol 87:e101–e107
40. Fujioka-Kobayashi M, Sawada K, Kobayashi E, Schaller B, Zhang Y, Miron RJ (2017) Osteogenic potential of rhBMP9 combined with a bovine-derived natural bone mineral scaffold compared to rhBMP2. Clin Oral Implants Res 28:381–387
41. Lamplot JD, Qin J, Nan G, Wang J, Liu X, Yin L, Tomal J, Li R, Shui W, Zhang H, Kim SH, Zhang W, Zhang J, Kong Y, Denduluri S, Rogers MR, Pratt A, Haydon RC, Luu HH, Angeles J, Shi LL, He TC (2013) BMP9 signaling in stem cell differentiation and osteogenesis. Am J Stem Cells 2:1–21
42. Liao J, Wei Q, Zou Y, Fan J, Song D, Cui J, Zhang W, Zhu Y, Ma C, Hu X, Qu X, Chen L, Yu X, Zhang Z, Wang C, Zhao C, Zeng Z, Zhang R, Yan S, Wu T, Wu X, Shu Y, Lei J, Li Y, Luu HH, Lee MJ, Reid RR, Ameer GA, Wolf JM, He TC, Huang W (2017) Notch signaling augments BMP-9-induced bone formation by promoting the osteogenesis-angiogenesis coupling process in mesenchymal stem cells (MSCs). Cell Physiol Biochem 41:1905–1923
43. Tang N, Song WX, Luo J, Luo X, Chen J, Sharff KA, Bi Y, He BC, Huang JY, Zhu GH, Su YX, Jiang W, Tang M, He Y, Wang Y, Chen L, Zuo GW, Shen J, Pan X, Reid RR, Luu HH, Haydon RC, He TC (2009) BMP-9 induced osteogenic differentiation of mesenchymal progenitors requires functional canonical Wnt/beta-catenin signaling. J Cell Mol Med 8B:2448–2464
44. Kang Q, Song WX, Luo Q, Tang N, Luo J, Luo X, Shen J, Bi Y, He BC, Park JK, Jiang W, Tang Y, Huang J, Su Y, Zhu GH, He Y, Yin H, Hu Z, Wang Y, Chen L, Zuo GW, Pan X, Shen J, Vokes T, Reid RR, Haydon RC, He TC (2009) A comprehensive analysis of the dual roles of BMPs in regulating adipogenic and osteogenic differentiation of mesenchymal progenitor cells. Stem Cells Dev 18:545–559
45. Li XL, Liu YB, Ma EG, Shen WX, Li H, Zhang YN (2015) Synergistic effect of BMP9 and TGF-β in the proliferation and differentiation of osteoblasts. Genet Mol Res 14:7605–7615
46. Zhao YF, Xu J, Wang WJ, Wang J, He JW, Li L, Dong Q, Xiao Y, Duan XL, Yang X, Liang YW, Song T, Tang M, Zhao D, Luo JY (2013) Activation of JNKs is essential for BMP9-induced osteogenic differentiation of mesenchymal stem cells. BMB Rep 46:422–427
47. Eiraku N, Chiba N, Nakamura T, Amir MS, Seong CH, Ohnishi T, Kusuyama J, Noguchi K, Matsuguchi T (2019) BMP9 directly induces rapid GSK3-β phosphorylation in a Wnt-independent manner through classIPI3K-Akt axis in osteoblasts. FASEB J 33:12124–12134
48. Wang Y, Hong S, Li M, Zhang J, Bi Y, He Y, Liu X, Nan G, Su Y, Zhu G, Li R, Zhang W, Wang J, Zhang H, Kong Y, Shui W, Wu N, He Y, Chen X, Luu HH, Haydon RC, Shi LL, He TC, Qin J (2013) Noggin resistance contributes to the potent osteogenic capability of BMP9 in mesenchymal stem cells. J Orthop Res 31:1796–1803
49. Nakamura T, Shinohara Y, Momozaki S, Yoshimoto T, Noguchi K (2013) Co-stimulation with bone morphogenetic protein-9 and FK506 induces remarkable osteoblastic differentiation in rat dedifferentiated fat cells. Biochem Biophys Res Commun 440:289–294
50. Yoshimaki T, Sato S, Kigami R, Tsuchiya N, Oka S, Arai Y, Ito K (2014) Bone regeneration by lactoferrin in non-critical-sized rat calvarial bone defects. J Med Biol Eng 34:256–260
51. Khadra M, Kasem N, Haanaes HR, Ellingsen JE, Lyngstadaas SP (2004) Enhancement of bone formation in rat calvarial bone defects using low-level laser therapy. Oral Surg Oral Med Oral Pathol Oral Radiol Endod 97:693–700
52. Pellegrini G, Seol YJ, Gruber R, Giannobile WV (2009) Preclinical models for oral and periodontal reconstructive therapies. J Dent Res 88:1065–1076

Publisher's note Springer Nature remains neutral with regard to jurisdictional claims in published maps and institutional affiliations.